Studies of High Energy Ions in Heliotron J

S. Kobayashi 1), H. Okada 1), M. Kaneko 2), Y. Suzuki 2), T. Mizuuchi 1), K. Nagasaki 1), Y. Nakamura 2), T. Takemoto 2), S. Murakami 3), S. Yamamoto 1), K. Kondo 2), K. Hanatani 1), F. Sano 1)

1) Institute of Advanced Energy, Kyoto University, Gokasho, Uji 611-0011, Japan
2) Graduate School of Energy Science, Kyoto University, Gokasho, Uji 611-0011, Japan
3) Graduate School of Engineering, Kyoto University, Kyoto 606-8501, Japan

e-mail contact of main author: kobayashi@iae.kyoto-u.ac.jp

Abstract. In order to investigate the effect of the magnetic field components on the energetic particle confinement in helical-axis heliotron configuration, the NBI and ICRF heating experiments have been carried out in Heliotron J with changing the mirror ripple component of the magnetic field. By scanning the charge exchange (CX) neutral particle analyzer (NPA) in the toroidal direction, it is found that the CX flux in NBI plasmas decreases with increasing the mirror ripple component when the toroidal angle of CX-NPA set perpendicularly, which can be interpreted by the change in the loss cone shape predicted by a theoretical calculation. The 1/e decay time of the CX flux for the tangentially injected beam ions, on the other hand, increases with the mirror ripple. In the ICRF minority heating experiment, it is found that the tail temperature of the minority ion increases with the ICRF power. The high energy minority ion up to 8 keV is observed only in the higher mirror ripple configurations. These results suggest that the configuration with higher mirror ripple is favorable for the confinement of the passing particles in this experimental condition.

1. Introduction

Energetic particle confinement is an important issue in toroidal devices for effective auxiliary heating or ignition [1,2]. In heliotron/stellarator systems, as compared with tokamaks, the asymmetry of the magnetic configuration due to its three-dimensional structure causes a serious energetic particle loss. To resolve this problem, the magnetic axis was shifted inwardly in the planar axis heliotron configurations, such as LHD, CHS and Heliotron E [3,4]. The particle confinement was improved in the inward-shifted configuration, while MHD modes were destabilized because of an enhancement of the magnetic hill.

The helical-axis heliotron device, Heliotron J, using the quasi-isodynamic (omnigeneous) magnetic configuration, is developed to minimize the loss of bounce averaged drift orbits at high beta [5]. The numerical analysis predicted that one of the magnetic Fourier components, mirror ripple, being the variation of the field strength along the toroidal direction, had a key role on the collisionless particle confinement in the helical-axis heliotron configuration [6]. Therefore, it is an urgent subject to verify the effect of the mirror ripple component on the particle confinement. It is also expected that the gap between the drift orbit and flux surface improves with increasing the plasma beta, which has a contribution to improve the energetic particle confinement in helical-axis heliotron configuration. In this study, we investigate the production and confinement of the energetic ions in Heliotron J with regard to the following subjects:

1. In order to examine the confinement properties of energetic ions in a collisionless regime, the hydrogen neutral beam (NB) was injected into the relatively low density deuterium plasmas ($<1\times10^{19}$ m^{-3}). The NBI system was installed to Heliotron J in 2003 for the sake of heating plasmas and producing high energy ions. Dependence of the mirror ripple component of the configuration on the energetic ion confinement was investigated by

scanning the mirror ripple without changing the major configuration properties, that is, the plasma axis, volume and radial profile of the rotational transform were fixed in the experiments. The charge exchange (CX) neutral particle analyzer (NPA) was used and scanned in poloidal and toroidal direction simultaneously to measure the pitch angle distribution of the CX neutrals. A particle orbit calculation for the ion guiding center was performed to discuss the experimental result.

2. ICRF heating is one of effective tools to generate energetic ions using minority heating scheme. This method does not bring particle source and there is no acceleration limit in practical sense since it is restricted only by confinement of fast ions. ICRF heating system was installed in the end of 2003 to investigate heating and confinement of energetic ions behavior. First of all, the plasma loading impedance of a loop antenna was investigated, and then the production and confinement of energetic ions were studied using CX-NPA in relation to injection power and magnetic configurations.

2. Neutral Beam Injection Experiment with Controlling Mirror Ripple Component

The NBI system installed in Heliotron J has two bucket-type ion sources whose maximum beam power and acceleration voltage are 0.7 MW and 30 keV in a tangential direction. Figure 1 illustrates a schematic view of the Heliotron J plasma boundary including heating and diagnostic systems. The CX-NPA system can measure the hydrogen and deuterium neutral fluxes separately. This system also has a capability to scan both poloidal (θ_{NPA}) and toroidal (ϕ_{NPA}) angles with the ranges of $-3^{\circ} < \theta_{NPA} < +10^{\circ}$ and $-10^{\circ} < \phi_{NPA} < +18^{\circ}$. The initial plasma is produced by 2nd harmonic 70 GHz ECH with a maximum injection power of 0.4 MW.

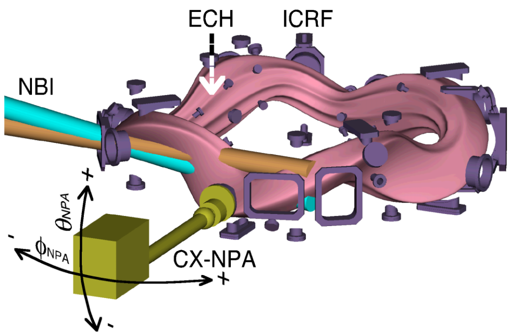

Fig. 1. Schematic view of the Heliotron J including heating and diagnostic systems.

In order to examine the effect of the mirror ripple on the energetic ion confinement in Heliotron J, we have carried out the mirror ripple control experiment. The mirror ripple component (B_{04}/B_{00}) at normalized minor radius ρ = 0.5 is varied from 0.02 to 0.16, where B_{mn} is the poloidal/toroidal mode numbers of magnetic field strength. In these configurations, the magnetic axis position ($\langle R_{ax}\rangle$ = 1.2 m), plasma volume (V_P = 0.7 m^3), radial profile of the rotational transform ($\iota/2\pi$ = 0.56 at LCFS) are kept constant. Moreover, another main Fourier component, the toroidal component normalized by the helical component (B_{10}/B_{14}) is almost unchanged. The upper three figures shown in Figs. 2(a)-(c) illustrate the magnetic field strengths at ρ = 0.52 along a field line in one poloidal period in the cases of B_{04}/B_{00} = 0.16, 0.07 and 0.02, respectively. The strength of the mirror ripple for the standard configuration of Heliotron J corresponds to 0.07. In the case for B_{04}/B_{00} = 0.16, the ripple amplitude is higher than the others, the minimum values of field strength at the bottoms of the mirror ripple are relatively flat. In contrast, in the configuration with the mirror ripple of 0.02, the strength of the ripple bottoms varies along the field line. The contour plots of the magnetic field strength are also shown in Figs. 2(a)-(c). The degree of alignment between the field line and $\nabla\mathbf{B}$ improves with increasing the mirror ripple component. It is hence expected that the difference between flux surface and drift orbits by $\nabla\mathbf{B}$ drift becomes smaller in the higher ripple configuration.

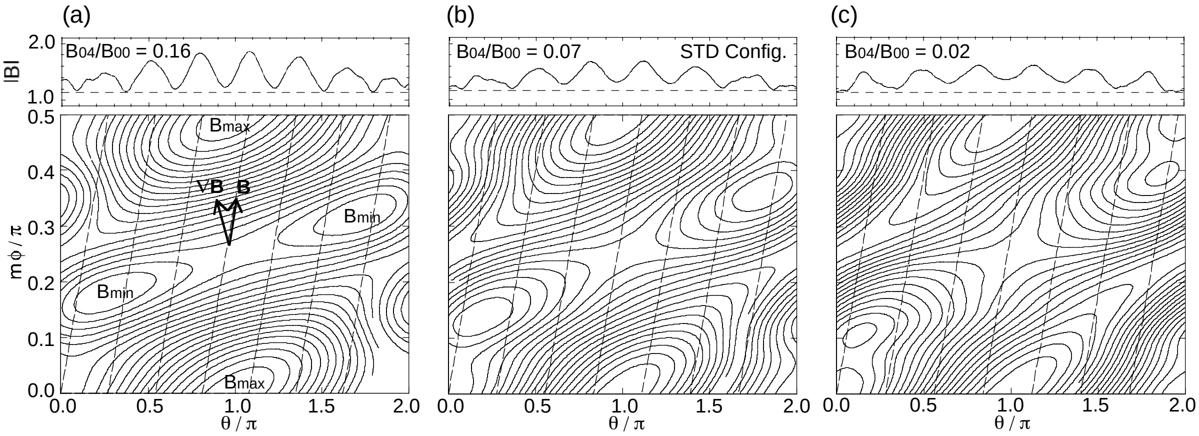

Fig. 2. Poloidal profiles of |B| along a field line (upper) and contour plots of |B| (lower) at ρ = 0.52 in the Boozer co-ordinates in the cases that the mirror ripple components (B_{04}/B_{00}) are (a) 0.16, (b) 0.07 and (c) 0.02, respectively. Each magnetic field line is represented by dashed line.

The CX flux was measured in the NBI heated plasmas by changing the mirror ripple component. To measure the pitch angle distribution of energetic ions, the toroidal angle of the CX-NPA was varied from ϕ_{NPA} = -3 º to +12 º. The poloidal angle of NPA was also adjusted so as to observe the chord across the magnetic axis in each toroidal angle. This scan enables us to measure a range of the pitch angle from 107º in the end of the mirror section and 130º in the straight section. The energy spectra of hydrogen CX flux are illustrated in Figs. 3(a)-(c) with the variation of the NPA toroidal angle. These data were obtained in the NBI plasmas in the same three configurations as shown in Fig. 2. The averaged electron density and acceleration voltage and injection power of NB (E_b) were to be 0.8×10^{19} m^{-3}, 27.4 kV and 0.5MW, respectively. In all the configurations, the beam energy components (E_b, $E_b/2$ and $E_b/3$) can be observed when CX-NPA is oriented to the beam-facing direction to ϕ_{NPA} = +12º. In the case of mirror ripple at 0.07, the full energy beam component can be seen even at ϕ_{NPA} = +6º. At the high ripple configuration, on the other hand, significant increase in the CX flux around the full energy is not confirmed at ϕ_{NPA} = +6º. Moreover the strength of the high energy (> 5 keV) CX flux at ϕ_{NPA} = 0º and +6º in the STD configuration is much higher than that for B_{04}/B_{00} = 0.16 case by a factor of more than 4. It is observed that there is no clear difference in the energy spectra between the STD and lower ripple configurations. In order to understand the experimental results, a non-collisional orbit calculation for ion guiding center was carried out. In this code, the ion orbit can be followed using the drift equation in the cylindrical co-ordinates until it strikes the wall. The loss time of the test particle having initial energy of 6.6 keV is shown in Figs. 4(a)-(c) for B_{04}/B_{00} = 0.16, 0.07 and 0.02 cases, respectively. In this calculation, the test particles were launched on the chord of CX-NPA with changing the radial position and the detection angle. In the configurations of B_{04}/B_{00} =

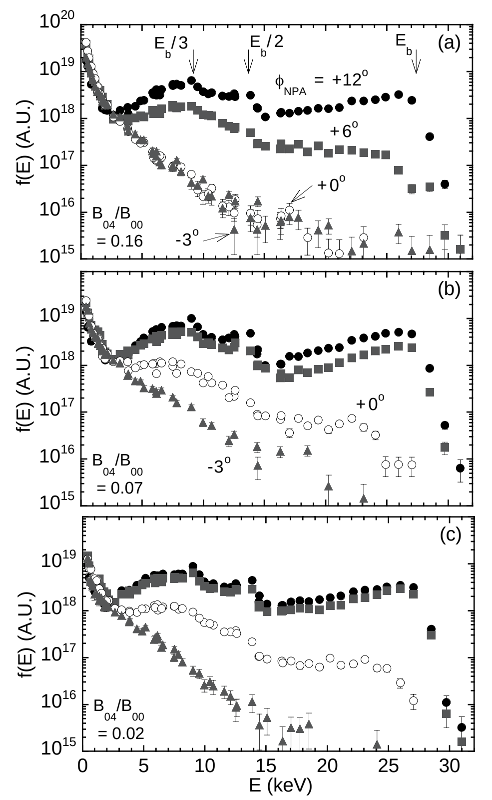

Fig. 3. Energy spectra for hydrogen CX flux obtained in the same three configurations as shown in Fig. 2.

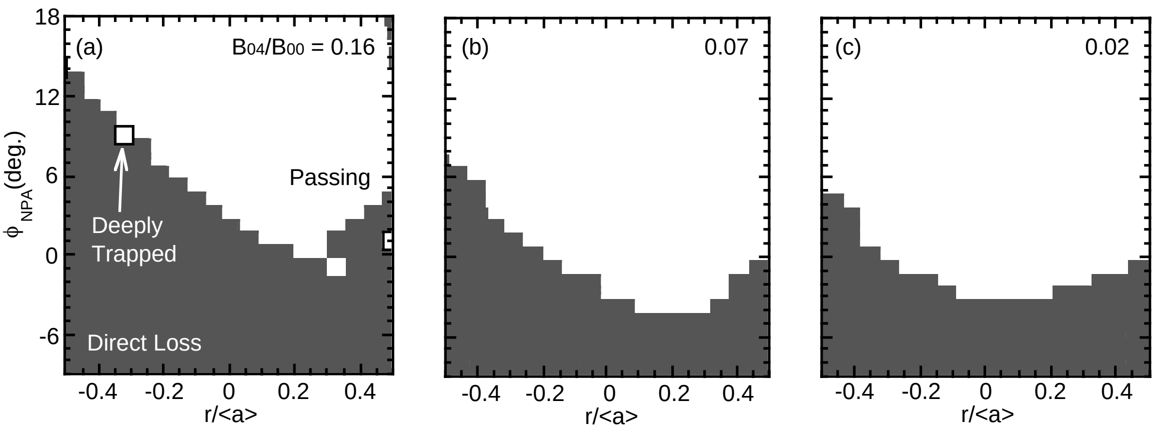

Fig. 4. Orbit following time of the non-collisional orbit calculation for proton (E = 6.6 keV) in B_{04}/B_{00} = (a) 0.16, (b) 0.07 and (c) 0.02 cases. The "Passing" particle has orbit following time longer than 5 ms and "Direct Loss" is for less than 0.5 ms.

0.07 and 0.02, the calculation predicts that CX-NPA at $\phi_{NPA} = 0^o$ can observe the passing particles, whose loss time is longer than 5 ms. For the higher mirror ripple configuration (B_{04}/B_{00} = 0.16), on the other hand, the main part of the detection area of CX-NPA at $\phi_{NPA} = 0^o$ is dominated by the direct loss (< 0.5 ms). In the cases for the STD and lower ripple configurations, the shapes of the loss cone are similar to each other, which is almost consistent with the experimental result. The change in the CX flux on the mirror ripple can be interpreted by the change in the loss cone shape and it is roughly determined by the depth of the mirror ripple.

The decay time of the CX flux just after NB turned-off provides information regarding the slowing down and the confinement time of the beam ions. Figure 5 shows the time evolution of the CX flux (E = 18 keV) after the NB turned-off for B_{04}/B_{00} = 0.16, 0.07 and 0.02 cases. The NPA toroidal angle was set to be +12^o to measure the CX flux having more similar pitch angle to the tangentially injected beam ions. The difference in the pitch angle of the detected ions among three configurations is less than 2^o. A clear dependence of the decay of the CX flux on the mirror ripple just after the NB turned-off is found, i.e. the 1/e decay time of the CX flux increases with the mirror ripple component. The orbit calculation predicts that the averaged loss rate, defined by the fraction of the numbers of the direct loss particles to the total test particles including deeply trapped and passing particles, is estimated to be 29% in the higher ripple configuration and 25% for the lower ripple case, under the condition that the initial energy and start point are 18 keV and ρ = 0.25, respectively. The On the basis of the classical theory for slowing-down of injected beam ions, the decay time of the CX flux decelerated from the injected energy just after the NB turned-off is roughly estimated from the expression given by Stix [7], as follows,

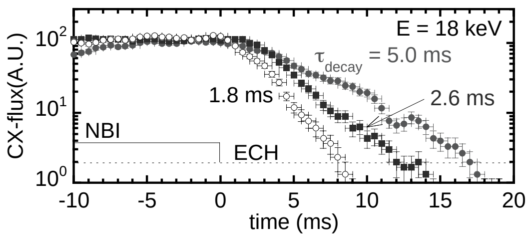

Fig. 5. Time evolution of the CX flux (E = 18 keV) just after the NB turned-off for B_{04}/B_{00} = 0.16 (●), 0.07 (■) and 0.02 (○) respectively.

$$\tau^*\left(E_{\text{inj}} \rightarrow E_{\text{det}}\right) = \frac{\tau_{\text{se}}}{3}\ln\left[\frac{1+\left(E_{\text{inj}}/E_{\text{c}}\right)^{3/2}}{1+\left(E_{\text{det}}/E_{\text{c}}\right)^{3/2}}\right],$$

where E_{inj}, E_{det} and E_c is the injected, detection and critical energy, respectively. Under the experimental condition, the slowing-down time τ_{se} is to be about 4.5 ms using the Spitzer's slowing-down time on the assumption that the effective charge is two, which is almost consistent with the experimental data for the higher mirror ripple case. Although the further analysis is needed with the calculation taking into account of the beam deposition and collision processes, these results suggest that the higher mirror ripple configuration is favorable for the confinement of the energetic passing ions.

3. First ICRF Minority Heating Experiment

3.1 Configuration and the Plasma Loading in ICRF Experiment

The minority heating experiment using H-minority and D-majority was performed in order to study the ICRF heating mechanism and high energy ion behavior in a helical-axis heliotron device, Heliotron J, using a loop antenna installed in the corner section where the mod-B surface is a talamak-like structure. The field structure and resonance/cut-off layers are shown in Fig. 6. The ICRF frequency of 19 MHz corresponds to the fundamental resonance for protons near the axis and 23.2 MHz corresponds to that at about 0.5 in the normalized minor radius in the STD configuration. The RF power was radiated from the antenna on the low field side to ECH target plasmas. The ECH power is in the range of 300 to 350 kW. Plasma resistance was investigated using an RF-current pickup coil and an RF-voltage detector installed in the co-axial transmission line between the matching circuit and the antenna. The antenna resistance due to the plasma loading was 1.5 to 5.0 ohms in the density range of 0.15 to 0.6×10^{19} m^{-3} as shown in Fig. 7. The calculated value using a fast wave model is also indicated by the solid line. Experimental values almost agree with the expected ones by the model calculation, where the plasma is assumed to be one-dimensional plane and the antenna is modeled as a three-dimensional current sheet with a infinite Faraday screen [8].

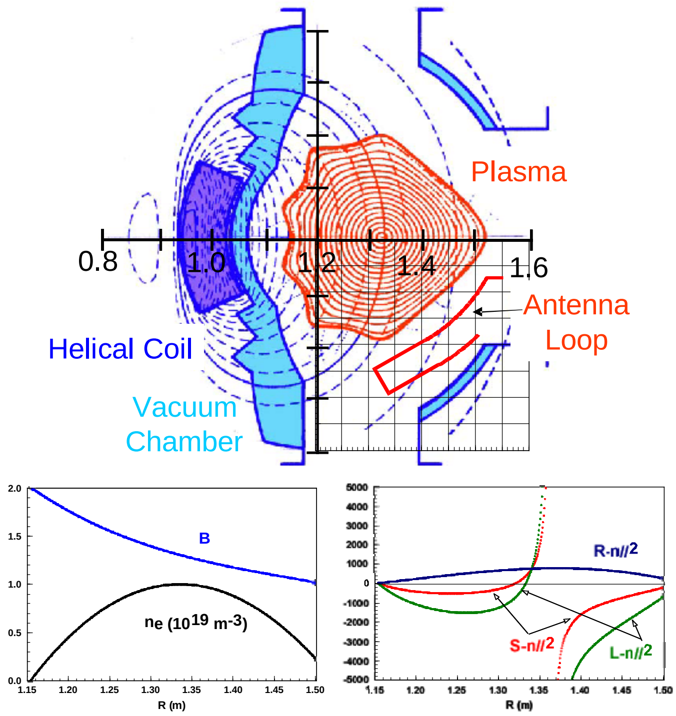

Fig. 6. Field configuration and antenna position (top), the magnetic field strength along the major radius (left), and the cold dispersion relation along the major radius (right).

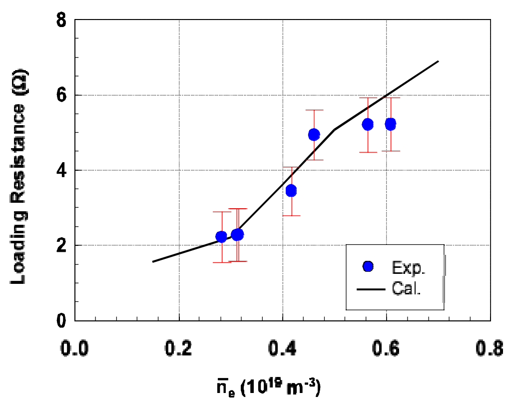

Fig. 7. Measured plasma loading resistance as a function of the density. The calculated values from the numerical model are also shown as the line.

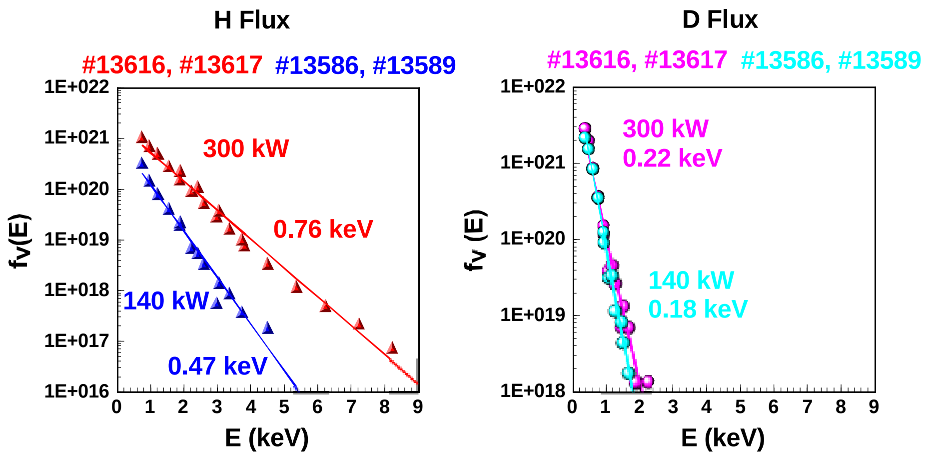

Fig. 8. Energetic proton spectra in the cases of the injection power of 300 kW and 140 kW (Left). Bulk deuteron spectra in the two cases of the left figure (Right).

3.2 Energetic Proton Production by ICRF Heating

Energetic proton flux was measured using the CX-NPA installed at the opposite toroidal position against the antenna position. In minority heating, the RF power is absorbed mainly by minority ions. It is considered that the energetic tail is one of the indexes of the heating. Observed proton and deuteron fluxes for the different injection power are shown in Fig, 8. The proton tail temperatures estimated from the energy spectra from the energy CX flux of 2-4.5 keV were 0.76 keV in the case of injection power of 300 kW, and 0.47 keV in the case of 140 kW. The tail temperature was increased as the injection power was increased although the bulk ion temperature kept its value of 0.2 keV during ICRF pulse (about 10 msec). The decay time of the flux after the ICRF pulse termination was short (about 1 msec) compared with the slowing down time and energy transfer time. It is considered that the orbit loss is not negligible for the ICRF heating in this low density condition. The spectrum dependence on the magnetic filed configuration was also investigated. The mirror ripple component was changed by controlling the ratio of the coil current of toroidal coil A (TA) to that of toroidal coil B (TB). Figure 9 shows the proton fluxes in the cases of STD (B_{04}/B_{00} = 0.07) and B_{04}/B_{00} = 0.02. ICRF injection power was 140 kW in the STD case, and 180 kW in the case of B_{04}/B_{00} = 0.02, respectively. The slope of the spectrum was steeper in the B_{04}/B_{00} = 0.02 case, that is, the energetic ion production was more effective in the STD case. The perpendicularly accelerated protons by ICRF heating were confined better in the STD configuration than in the lower mirror ripple configuration. The higher mirror ripple configuration, therefore, is preferable for ICRF heating in this experimental condition.

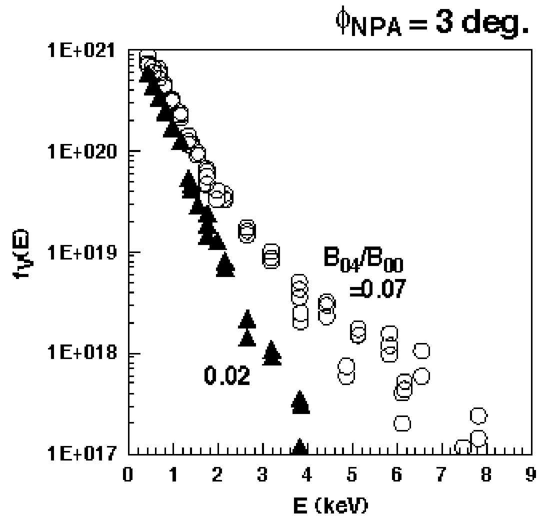

Fig. 9. Energetic proton spectra in the two magnetic configurations during ICRF heating.

4. Conclusions

The NBI and ICRF heating experiments have been successfully started in Heliotron J from 2003. The effect of the magnetic field component, mirror ripple, on the particle confinement has been investigated experimentally by changing the mirror ripple component with keeping the other configuration characteristics, in especially magnetic axis, almost constant.

By scanning CX-NPA in the toroidal direction, it is found that the CX flux in NBI plasmas decreases with increasing the mirror ripple component when the NPA toroidal angle is set perpendicularly. The non-collisional orbit calculation has been performed to understand the experimental result. The calculation predicts that the dependence of the CX flux on the mirror ripple is due to the change in the loss cone shape. The 1/e decay time of the CX flux for the tangentially injected beam ion increases with the mirror ripple, the direct loss rate from the calculation, on the other hand, has no clear difference among these configurations.

In the ICRF minority heating experiment, the proton tail temperature increases with the ICRF injection power up to 0.76 keV, while the bulk temperature is almost unchanged. The high energy minority tail up to 8 keV is observed only in the higher mirror ripple configuration.

These results suggest that the configuration with higher mirror ripple may have an effect to improve the confinement of the passing particles in these experimental conditions. The investigation of the beta effect on the improvement in energetic particle confinement is future work in Heliotron J.

Acknowledgement

The authors would like to thank the members of the Heliotron J group for their helpful suggestions and supports in the experiments. The authors are also obliged to the CHS group at the National Institute for Fusion Science for fruitful discussions. This work is partly supported by a Grant-in-Aid for Scientific Research from the Ministry of Education, Culture, Sports, Science and Technology No. 15760621 and by the 21st Century program of Establishment of COE on Sustainable-Energy System from the Japan Society for the Promotion of Science.

References

[1] HEIDBRINK, W. W. et al., Nucl. Fusion **34** (1994)535.
[2] ITER Physics Expert Group on Energetic Particles, Heating and Current Drive Expert Group, ITER Physics Basic Editors, Nucl. Fusion **36** (1999) 2471.
[3] OBIKI, T. et al., 13th International Conference on Plasma Physics and Controlled Nuclear Fusion Research, 1990, Vol. 2 IAEA-CN-53 (1991) 425.
[4] OKAMURA, S. et al., Nucl. Fusion **39** (1999) 1337.
[5] OBIKI, T. et al., Nucl. Fusion **41** (2001) 833.
[6] YOKOYAMA, M. et al., Nucl. Fusion **40** (2000) 261
[7] STIX, T. H., Plasma Phys. **14** (1972) 367.
[8] THEILHABER, K. and JACQUINOT, J., Nucl. Fusion **24** (1984) 541.